

Configurational Multiplicity of Porphyrin  $\pi$  Cation Radicals: Nickel  $\pi$ - $\pi$  Dimers

Kathleen M. Barkigia, Mark W. Renner, and Jack Fajer\*

Department of Applied Science, Brookhaven National Laboratory, Upton, New York 11973-5000

Received: July 23, 1997<sup>⊗</sup>

The molecular structure of the Ni(II)OEP<sup>+</sup>ClO<sub>4</sub><sup>-</sup>  $\pi$  cation radical is reported (OEP = 2,3,7,8,12,13,17,18-octaethylporphyrin). The vibrational spectrum of a *single* crystal, recorded with an FT-IR microspectrometer, shows the <sup>2</sup>A<sub>1u</sub> HOMO occupancy marker band predicted for an OEP cation radical. The radical crystallizes as a cofacial  $\pi$ - $\pi$  dimer, (NiOEP<sup>+</sup>ClO<sub>4</sub><sup>-</sup>)<sub>2</sub>·2CH<sub>2</sub>Cl<sub>2</sub>, in an eclipsed configuration with the following parameters: mean interplanar separation = 3.36 Å, Ni-Ni = 3.41 Å, Ct-Ct = 3.46 Å, lateral shift = 0.83 Å, translational slip angle = 13.9°, and zero rotation of equivalent N-Ni-N axes. This dimeric configuration differs significantly from that of a related (NiOEP<sup>+</sup>ClO<sub>4</sub><sup>-</sup>)<sub>2</sub>·8CH<sub>2</sub>Cl<sub>2</sub> dimer and from those of several other metallo (M) OEP radical dimers described previously. The present results offer exceptions to generalizations recently proposed regarding the geometry and extent of  $\pi$ - $\pi$  interactions in fully and partially oxidized MOEP<sup>+</sup> dimeric  $\pi$  cation radicals such as (MOEP<sup>+</sup>)<sub>2</sub> and (MOEP)<sub>2</sub><sup>+</sup>. Indeed, the configuration and geometry of the (NiOEP<sup>+</sup>ClO<sub>4</sub><sup>-</sup>)<sub>2</sub> dimer reported here are more akin to those of a half-oxidized dimer (NiOEP)<sub>2</sub><sup>+</sup>SbCl<sub>6</sub><sup>-</sup> than to those of a fully oxidized (NiOEP<sup>+</sup>ClO<sub>4</sub><sup>-</sup>)<sub>2</sub> dimer reported previously (Scheidt et al. *Inorg. Chem.* **1996**, 35, 7500). The present results do demonstrate that identical porphyrin  $\pi$  cation radicals can aggregate in and adopt more than one unique cofacial geometry with different conformations,  $\pi$ - $\pi$  overlaps, and intermolecular spacings. Such multiple configurational architectures may help explain why the oxidized bacteriochlorophyll dimers (special pairs) of bacterial photosynthetic reaction centers exhibit varying unpaired spin density profiles.

## Introduction

Among synthetic porphyrins, the peripheral substituent pattern of 2,3,7,8,12,13,17,18-octaethylporphyrins (OEP) most closely resembles those of biological porphyrins and hydroporphyrins. Its derivatives thus serve as valuable paradigms for the  $\pi$ - $\pi$  interactions between the (bacterio)chlorophylls ((B)Chls) in light-harvesting and reaction center proteins, and for the radicals that evolve in the primary events of photosynthesis.<sup>1,2</sup> The common occurrence of porphyrinic  $\pi$  cation radical transients in bioenergetic catalysis<sup>3</sup> as well as in photosynthesis has naturally focused attention on the structural consequences of electron transfer and on the properties of the resulting  $\pi$  radicals.<sup>4,5</sup>

Crystallographic studies of isolated porphyrin  $\pi$  radicals have sought to model the stereochemical effects of the ubiquitous biological oxidations. In particular, Scheidt and co-workers<sup>6-8</sup> have attempted to develop general crystallographic trends and parameters for the dimeric  $\pi$ - $\pi$  aggregates of metallo (M) OEP radicals in their fully and half-oxidized states, (MOEP<sup>+</sup>)<sub>2</sub> and (MOEP)<sub>2</sub><sup>+</sup>, respectively. Structural descriptions of the latter are especially pertinent to the oxidized donors or special pairs of (B)Chls that result from the primary charge separation in photosynthetic organisms;<sup>2</sup> the model and biological radicals are formally at the same oxidation levels:<sup>8</sup> (MOEP)<sub>2</sub><sup>+</sup> and ((B)-Chl)<sub>2</sub><sup>+</sup>.

We report here the molecular structure of a Ni(II)OEP<sup>+</sup>ClO<sub>4</sub><sup>-</sup>  $\pi$  cation radical. The radical crystallizes as a cofacial  $\pi$ - $\pi$  dimer, (NiOEP<sup>+</sup>ClO<sub>4</sub><sup>-</sup>)<sub>2</sub>·2CH<sub>2</sub>Cl<sub>2</sub>, **1**, in an eclipsed configuration that differs significantly from that of a related (NiOEP<sup>+</sup>ClO<sub>4</sub><sup>-</sup>)<sub>2</sub>·8CH<sub>2</sub>Cl<sub>2</sub> dimer<sup>6</sup> and from those of several other Zn, Cu, and Fe OEP radical dimers<sup>4,6,7</sup> described previously.

The present results thus supplement or, at the very least, offer clear exceptions to the generalizations recently proposed<sup>6-8</sup> regarding the geometry and extent of  $\pi$ - $\pi$  interactions in fully and partially oxidized MOEP<sup>+</sup> dimeric  $\pi$  cation radicals.

The present results do establish that identical porphyrin  $\pi$  cation radicals can aggregate in and adopt more than one unique cofacial geometry with different  $\pi$ - $\pi$  overlaps and intermolecular spacings. Such multiple configurational architectures may help explain the two distinct unpaired spin density profiles for the oxidized special pair recently detected in the same photosynthetic bacterium<sup>9</sup> and the variety of spin profiles observed for the special pairs in different bacteria and in photosystems I and II of green plants and algae.<sup>2</sup>

In a related context, the infrared vibrational spectrum of a *single* crystal of the NiOEP<sup>+</sup> dimer has been recorded by FT-IR microspectroscopy. It clearly shows the <sup>2</sup>A<sub>1u</sub> HOMO occupancy marker band predicted for an OEP cation radical.<sup>10,11</sup>

## Experimental Section

NiOEP<sup>+</sup>ClO<sub>4</sub><sup>-</sup> (NiN<sub>4</sub>C<sub>36</sub>H<sub>44</sub><sup>+</sup>ClO<sub>4</sub><sup>-</sup>) was prepared by oxidation of Ni(II)OEP (Aldrich) with AgClO<sub>4</sub> in CH<sub>2</sub>Cl<sub>2</sub> in the presence of ~10<sup>-2</sup> M Bu<sub>4</sub>NClO<sub>4</sub>. The compound (NiOEP<sup>+</sup>ClO<sub>4</sub><sup>-</sup>)<sub>2</sub>·2CH<sub>2</sub>Cl<sub>2</sub> (**1**) crystallized from CH<sub>2</sub>Cl<sub>2</sub>/pentane in space group *P*2<sub>1</sub>/*n* with *a* = 10.824(1) Å, *b* = 29.431(3) Å, *c* = 11.766(3) Å,  $\beta$  = 98.33(1)°, *V* = 3708.6(11) Å<sup>3</sup>, and *Z* = 4. Data were collected at 200 K on an Enraf Nonius CAD4 diffractometer with Cu K $\alpha$  radiation in the range 4° ≤ 2 $\theta$  ≤ 130°. A total of 6969 reflections (*hk* ± *l*) were measured with 6129 unique. Refinement with SHELXL93 yielded *R*<sub>1</sub> = 0.062, *wR*<sub>2</sub> = 0.168 for *I* > 2 $\sigma$ (*I*) and *R*<sub>1</sub> = 0.122, *wR*<sub>2</sub> = 0.205 for all data. EPR spectra were recorded on a Bruker 200D spectrometer. FT-IR spectra of single crystals were obtained with an IR microspectrometer comprised of an integrated FT-IR spectrometer and microscope optical module (Spectra Tech).<sup>12</sup>

\* Address correspondence to this author. Fax: 516-344-3137. E-mail: fajerj@bnl.gov.

<sup>⊗</sup> Abstract published in *Advance ACS Abstracts*, October 1, 1997.

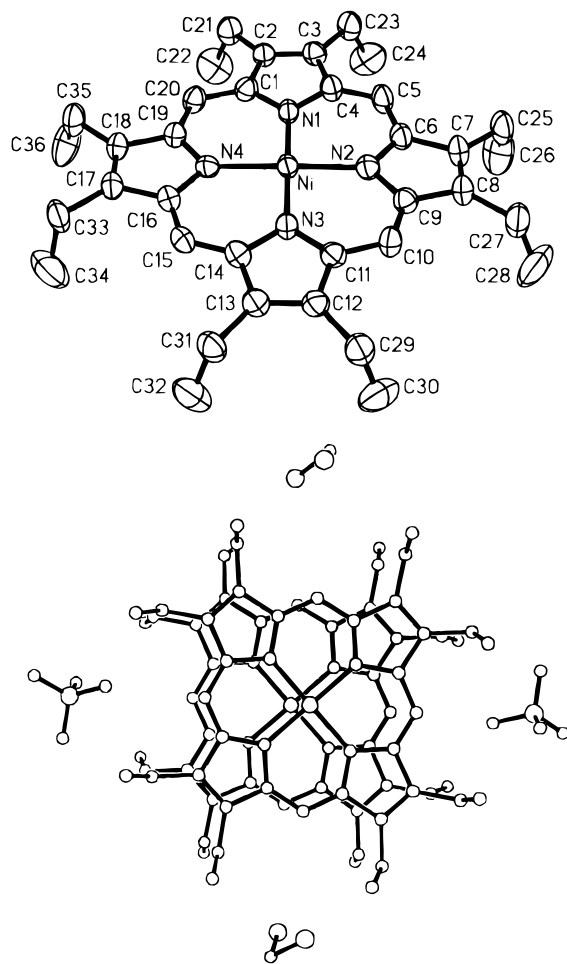
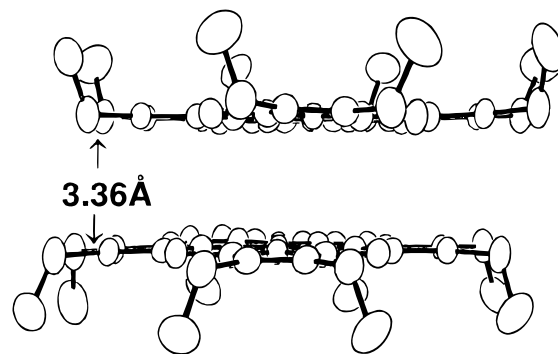


**Figure 1.** (Top) Molecular structure and atom names for one NiOEP<sup>+</sup> subunit. Thermal ellipsoids enclose 50% probability. (Bottom) Configuration of the dimer (NiOEP<sup>+</sup>ClO<sub>4</sub><sup>-</sup>)<sub>2</sub>·2CH<sub>2</sub>Cl<sub>2</sub> that includes the two ClO<sub>4</sub><sup>-</sup> counterions and the two CH<sub>2</sub>Cl<sub>2</sub> of solvation. Thermal ellipsoids are reduced to 1%. In top and bottom, hydrogens are omitted for clarity. Representative bond distances (Å): Ni–N = 1.945(4), N–C $\alpha$  = 1.384(6), C $\alpha$ –C $\beta$  = 1.455(7), C $\beta$ –C $\beta$  = 1.340(7), C $\alpha$ –C<sub>meso</sub> = 1.369(7), O<sub>3</sub>ClO<sup>-</sup> – C<sub>meso</sub> = 3.54(5).

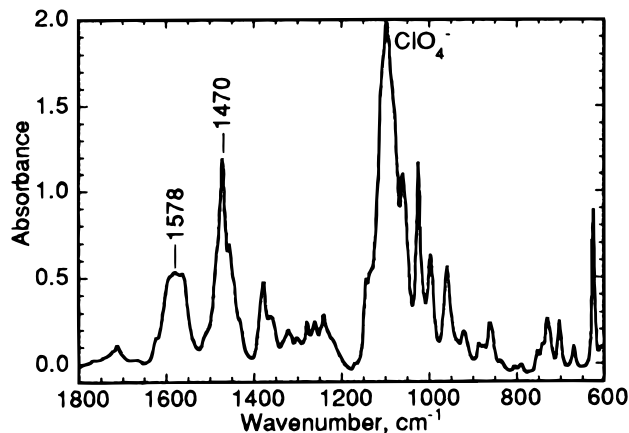
## Results

Figure 1 presents the molecular structure and atom names for one NiOEP<sup>+</sup> subunit of the dimeric (NiOEP<sup>+</sup>ClO<sub>4</sub><sup>-</sup>)<sub>2</sub>·2CH<sub>2</sub>Cl<sub>2</sub>. Figure 1 also illustrates the configuration of the latter as well as the placements of the two ClO<sub>4</sub><sup>-</sup> counterions and of the two CH<sub>2</sub>Cl<sub>2</sub> solvate molecules. Note that there is one counterion per porphyrin; i.e., each macrocycle has undergone a one-electron oxidation. Representative averaged bond distances are given in the figure legend, and a complete set of coordinates, bond distances and angles, and displacements from planarity is appended in the Supporting Information. The edge-on view of Figure 2 further illustrates the configuration of the dimer.

The porphyrin macrocycles remain essentially planar with the largest displacements from the average 24-atom plane less than 0.1 Å (−0.07, +0.06, and −0.07 Å at C2, C5, and C7, respectively.) The average Ni–N distances of 1.945(4) Å are also consistent with a planar porphyrin.<sup>4</sup> The separation between the mean planes (MPS) is 3.36 Å, a value typical of strong  $\pi$ – $\pi$  bonding.<sup>4,5</sup> The Ni ions are displaced 0.05 Å toward each other with Ni–Ni and center-to-center (Ct–Ct) distances of 3.41 and 3.46 Å, respectively. As shown in Figures 1 and 2, the two porphyrins form a slightly slipped, eclipsed configuration with parallel N–Ni–N axes, a lateral shift between centers of 0.83 Å, and a translational slip angle of 13.9°.



**Figure 2.** Edge-on view of the porphyrin radicals that comprise the dimer. The mean interplanar separation (MPS) of 3.36 Å is typical of strong  $\pi$ – $\pi$  interactions.



**Figure 3.** FT-IR spectrum obtained by microspectroscopy on a single crystal of (NiOEP<sup>+</sup>ClO<sub>4</sub><sup>-</sup>)<sub>2</sub>·2CH<sub>2</sub>Cl<sub>2</sub>.

The two major classes of synthetic porphyrins, OEPs and TPPs (5,10,15,20-tetraphenylporphyrin), lose an electron from different HOMOs when oxidized to form cation radicals.<sup>10</sup> In OEPs, the electron is abstracted from an  $a_{1u}$  orbital resulting in <sup>2</sup>A<sub>1u</sub> radicals (in  $D_{4h}$  symmetry) with unpaired spin density localized principally on the C $\alpha$ , and to a lesser extent on the C $\beta$  atoms. In contrast, TPPs lose an electron from an  $a_{2u}$  orbital yielding <sup>2</sup>A<sub>2u</sub> radicals with unpaired spin concentrated at the nitrogens and meso carbons.<sup>10</sup> The  $\pi$  cation radicals also exhibit diagnostic IR marker bands at 1550–1600 cm<sup>-1</sup> for OEPs and 1290–1300 cm<sup>-1</sup> for TPPs.<sup>11</sup> The IR marker bands thus also act as reporters of the orbital occupancy.<sup>6–8,11</sup> FT-IR spectra of single crystals of **1** were obtained by microspectroscopy, a technique that couples a microscope to a FT-IR spectrometer<sup>12</sup> and thus allows the recording of vibrational spectra of the same single crystals whose structures were determined crystallographically. The FT-IR spectrum of **1** is presented in Figure 3. The crystalline radical clearly absorbs in the region predicted for <sup>2</sup>A<sub>1u</sub> species with the characteristic marker bands attributed to C $\alpha$ –C<sub>meso</sub> and C $\beta$ –C $\beta$  stretches<sup>11</sup> centered at 1578 cm<sup>-1</sup>. (These bands are absent in all three known crystalline forms of the parent NiOEP.<sup>4,13</sup> Data for all the crystalline species are included in the Supporting Information. The prominent peaks at 1470 cm<sup>-1</sup> are CH<sub>2</sub> scissor bands.<sup>11</sup>)

In solution, NiOEP<sup>+</sup>ClO<sub>4</sub><sup>-</sup> exhibits an EPR signal typical of porphyrin  $\pi$  cation radicals.<sup>10</sup> However, single crystals of **1** display only a residual EPR signal (Figure 4). The close  $\pi$ – $\pi$  interactions in the dimers thus result in strong antiferromagnetic coupling between the spins of the two radicals and yield diamagnetic pairs. Similar couplings have been observed in several other MOEP<sup>+</sup> dimers.<sup>4–7,10</sup> Note that when the crystals

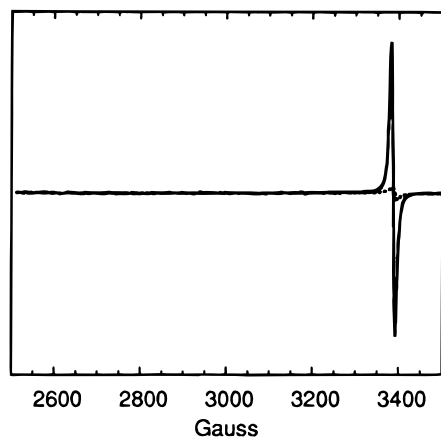


**Figure 4.** EPR spectra of a single crystal of the dimer (····) and of the same crystal dissolved in 0.1 mL of  $\text{CH}_2\text{Cl}_2$  (—).

of the dimer are redissolved, the EPR signal of the monomeric radical reappears (Figure 4).

A distinctive pattern of alternating short and long bond distances within the porphyrin inner  $\pi$  network comprised of the nitrogen, C $\alpha$ , and Cmeso atoms often accompanies the formation of magnetically coupled OEP $^+$  dimers.<sup>4,6,7</sup> This effect has been variously ascribed to a new type of intermolecular bonding<sup>4,6</sup> or to mixing of the  $a_{1u}/a_{2u}$  orbitals.<sup>14</sup> In the present case, although there are some bond alternations in the inner  $\pi$  system of the NiOEP $^+$ , these are not systematic and thus tend to exclude either significant orbital mixing or novel intermolecular bonding. In addition, unlike the previously reported (NiOEP $^+$ ClO $_4^-$ ) $_2$  in which the short Ni–Ni distance of 3.01 Å suggested a possible Ni–Ni  $\sigma$  bond<sup>6</sup>, the Ni–Ni distance of 3.41 Å in the present structure argues against such metal bonding interactions here.

Scheidt and co-workers have reported the structures of a series of MOEP $^+$  radicals consisting of fully or half-oxidized dimers, (MOEP $^+$ ) $_2$  and (MOEP) $_2^+$ , and have attempted to derive general trends that describe the  $\pi$ – $\pi$  interactions and architecture of these radicals.<sup>4,6–8</sup> Two of the configurations described by Scheidt et al. are shown in Figure 5. They depict the relative overlap of a fully oxidized (NiOEP $^+$ ) $_2$  dimer<sup>6</sup> and that of a half-oxidized (NiOEP) $_2^+$  dimer.<sup>8</sup> These generally represent the arrangements of several other MOEP $^+$  radicals as well, in which the average values of interplanar spacings, lateral shifts, and slip angles in (MOEP $^+$ ) $_2$  are typically smaller than in (MOEP) $_2^+$ .<sup>4,8</sup> However, the architecture and parameters of the (NiOEP $^+$ ) $_2$  dimer reported here resemble more closely those of the half-oxidized dimer,<sup>8</sup> (NiOEP) $_2^+$ , than those of the earlier fully oxidized (NiOEP $^+$ ) $_2$  dimer;<sup>6</sup> see Figure 5.

The present results thus demonstrate that identical  $\pi$  cation radicals can aggregate in more than one configuration. In addition, they offer, at the very least, a clear exception to the generalizations suggested by Scheidt and co-workers, and/or they require that additional factors that control the architecture of the dimers be considered. The most obvious differences between the two (NiOEP $^+$ ClO $_4^-$ ) dimers are the large number of solvate  $\text{CH}_2\text{Cl}_2$  molecules (eight) in the Scheidt structure<sup>6</sup> and the methods of oxidation and crystallization. In the present case, a large amount of  $\text{Bu}_4\text{NClO}_4$  was also present and thus imposed a significantly different ionic strength and polarity to the medium of crystallization than in the Scheidt method. The solvent polarity and high concentration of ClO $_4^-$  counterions may be particularly significant in that the dimerization requires that the two cationic radicals come together.<sup>15</sup> Note in Figure 1 that the two anions closely flank the cationic porphyrins: the distances from a perchlorate oxygen to the nearest porphyrin

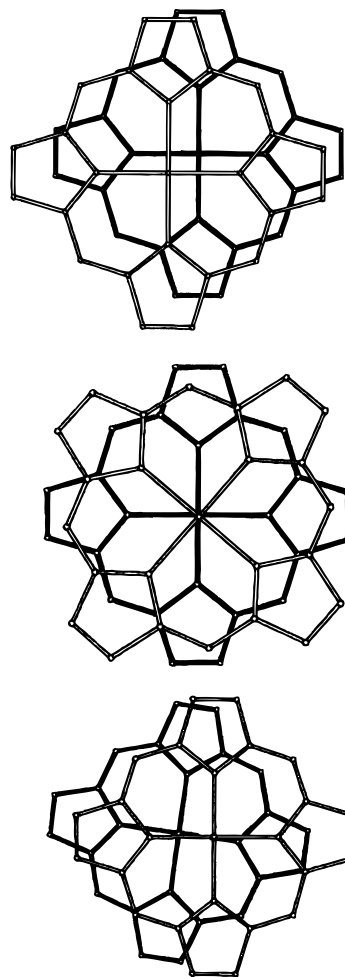


**Figure 5.** Relative porphyrin configurations in three dimeric NiOEP $^+$  radicals. (Top) (NiOEP $^+$ ClO $_4^-$ ) $_2$ ·2 $\text{CH}_2\text{Cl}_2$  reported here. MPS = 3.36 Å, Ct–Ct = 3.46 Å, Ni–Ni = 3.41 Å, lateral shift = 0.83 Å, translational slip angle = 13.9°. (Middle) (NiOEP $^+$ ClO $_4^-$ ) $_2$ ·8 $\text{CH}_2\text{Cl}_2$  from Song et al.<sup>6</sup> MPS = 3.19 Å, Ct–Ct = 3.08 Å, Ni–Ni = 3.01 Å, lateral shift = 0.0 Å, slip angle 0.0°. (Bottom) (NiOEP) $_2^+$ ·SbCl $_6^-$ · $\text{CH}_2\text{Cl}_2$  (half-oxidized dimer) from Scheidt et al.<sup>8</sup> MPS = 3.32 Å, Ct–Ct = 3.51 Å, Ni–Ni = 3.43 Å, lateral shift = 1.16 Å, slip angle = 19.4°.

meso carbons are only 3.49 and 3.58 Å. As well, the two  $\text{CH}_2\text{Cl}_2$  solvate molecules are well ordered, unlike several of the eight  $\text{CH}_2\text{Cl}_2$  in the Scheidt structure that are quite disordered.

These results may be particularly relevant to the recent report<sup>9</sup> that the oxidized special pairs, P $^+$ , in reaction centers of the photosynthetic bacterium *Rhodobacter sphaeroides* exhibit two distinct electronic configurations, as determined by ENDOR, that depend on the ionic nature of the detergents used to isolate the reaction centers.<sup>9</sup> The spin distributions (and optical spectra) of the two P $^+$  configurations clearly reflect different spacings and/or overlaps of the two bacteriochlorophylls that comprise the special pairs. (The spin distribution is delocalized ~2:1 between the two BChls in the “normal” P $^+$  and ~5:1 in the second configuration.<sup>9</sup>)

Obviously, the NiOEP $^+$  dimers are not exact paradigms for oxidized BChl special pairs. Nonetheless, the multiple configurations observed for the BChl and OEP radicals *do* establish that identical porphyrinic radicals can adopt more than one unique architecture in vivo as well as in vitro. Additional evidence against unique architectures for the special pairs in vivo was already suggested by the differences in  $\pi$ – $\pi$  stacking of P in *Rb. sphaeroides* and *Rhodospseudomonas viridis*<sup>1</sup> and by the differences in spin delocalization found in their “normal” oxidized special pairs.<sup>2,9,16</sup>

Unlike photosynthetic bacteria, green plants and algae function via two photosystems whose primary chlorophyll donors, P680 and P700, exhibit very different redox and spectral properties variously attributed to monomeric and/or dimeric chlorophylls.<sup>2,16,17</sup> Extrapolation of the above results and discussion prompts us to suggest that variations in architecture and  $\pi$ - $\pi$  overlap resulting from relatively small changes in the protein scaffoldings that hold the chromophores would also provide very simple mechanisms for modulating the properties of "dimeric" P680 and P700.<sup>2,16,17</sup>

**Acknowledgment.** We thank L. Carr, L. M. Miller and G. P. Williams for their assistance with the FT-IR microspectroscopy. This work was supported by the Division of Chemical Sciences, U.S. Department of Energy, under Contract DE-AC02-76CH00016.

**Supporting Information Available:** Details of the crystallographic data collection and refinement; figures of bond distances and displacements from planarity; comparison of the FT-IR spectra of **1** and of three crystalline forms of NiOEP; tables of positional and thermal parameters for the atoms of **1** and of bond distances and angles (10 pages). Ordering information is given on any current masthead page.

## References and Notes

- (1) Prince, S. M.; Papiz, M. Z.; Freer, A. A.; McDermott, G.; Hawthornthwaite-Lawless, A. M.; Cogdell, R. J.; Isaacs, N. W. *J. Mol. Biol.* **1997**, *268*, 412. Ermler, V.; Fritsch, G.; Buchanan, S. K.; Michel, H. *Structure* **1994**, *2*, 925. Deisenhofer, J.; Epp, O.; Sinning, I.; Michel, H. *J. Mol. Biol.* **1995**, *246*, 429.
- (2) For a review, see: Bixon, M.; Fajer, J.; Feher, G.; Freed, J. H.; Gamliel, D.; Hoff, A. J.; Levanon, H.; Möbius, K.; Nechushtai, R.; Norris, J. R.; Scherz, A.; Sessler, J. L.; Stehlik, D. *Isr. J. Chem.* **1992**, *32*, 369.
- (3) Sono, M.; Roach, M. P.; Coulter, E. D.; Dawson, J. H. *Chem. Rev.* **1996**, *96*, 2841. Sundaramoorthy, M.; Kishi, K.; Gold, M. H.; Poulos, T. L. *J. Biol. Chem.* **1994**, *269*, 32759. Ravichandran, K. G.; Boddupalli, S. S.; Hasemann, C. A.; Peterson, J. A.; Deisenhofer, J. *Science* **1993**, *261*,

731. Crane, B. R.; Siegel, L. M.; Getzoff, E. D. *Science*, **1995**, *270*, 59. Chang, C. K.; Hanson, L. K.; Richardson, P. F.; Young, R.; Fajer, J. *Proc. Natl. Acad. Sci. U.S.A.* **1981**, *78*, 2652. Dolphin, D.; Forman, A.; Borg, D. C.; Fajer, J.; Felton, R. H. *Proc. Natl. Acad. Sci. U.S.A.* **1971**, *68*, 614.
- (4) Scheidt, W. R.; Lee, J. H. *Struct. Bonding (Berlin)* **1987**, *64*, 1.
- (5) Barkigia, K. M.; Fajer, J. In *The Photosynthetic Reaction Center*; Deisenhofer, J., Norris, J. R., Eds.; Academic Press: San Diego, CA, 1993; Vol. II, p 513.
- (6) Song, H.; Orosz, R. D.; Reed, C. A.; Scheidt, W. R. *Inorg. Chem.* **1990**, *29*, 4274.
- (7) Schultz, C. E.; Song, H.; Mislankar, A.; Orosz, R. D.; Reed, C. A.; Debrunner, P. G.; Scheidt, W. R. *Inorg. Chem.* **1997**, *36*, 406 and references therein.
- (8) Scheidt, W. R.; Brancato-Buentello, K. E.; Song, H.; Reddy, K. V.; Cheng, B. *Inorg. Chem.* **1996**, *35*, 7500.
- (9) Müh, F.; Rautter, J.; Lubitz, W. *Biochemistry* **1997**, *36*, 4155 and references therein.
- (10) Fajer, J.; Davis, M. S. *The Porphyrins*; Dolphin, D., Ed.; Academic Press: New York, 1979; Vol. IV, p 197.
- (11) Shimomura, E. T.; Phillippi, M. A.; Goff, H. M.; Scholz, W. F.; Reed, C. A. *J. Am. Chem. Soc.* **1981**, *103*, 6778. Hu, S.; Spiro, T. G. *J. Am. Chem. Soc.* **1993**, *115*, 12029.
- (12) Reffner, J. A.; Martoglio, P. A.; Williams, G. P. *Rev. Sci. Instrum.* **1995**, *66*, 1298.
- (13) Meyer, E. F., Jr. *Acta Crystallogr., Sect. B* **1974**, *B28*, 2162. Cullen, D. L.; Meyer, E. F., Jr. *J. Am. Chem. Soc.* **1974**, *96*, 2095. Brennan, T. D.; Scheidt, W. R.; Shelnutt, J. A. *J. Am. Chem. Soc.* **1988**, *110*, 3919.
- (14) Sibilila, S. A.; Hu, S.; Piffat, C.; Melamed, D.; Spiro, T. G. *Inorg. Chem.* **1997**, *36*, 1013.
- (15) These conclusions are supported further by two structures of MgOEP<sup>+</sup> radicals reported very recently. One of these conforms to the "standard" (MOEP<sup>+</sup>)<sub>2</sub> Scheidt dimer. The other, crystallized at a different solvent polarity, consists effectively of two monomeric radicals that overlap only at the periphery of one pyrrole ring. Brancato-Buentello, K. E.; Scheidt, W. R. *Angew. Chem., Int. Ed. Engl.* **1997**, *36*, 1456.
- (16) Möbius, K.; Lubitz, W.; Plato, M. In *Advanced EPR*; Hoff, A. J., Ed.; Elsevier: Amsterdam; 1989; p 441. Lubitz, W. In *Chlorophylls*; Scheer, H., Ed.; CRC Press: Boca Raton, FL, 1991; p 903. Lubitz, W.; Lendzian, F. In *Biophysical Techniques in Photosynthesis*; Ames, J., Hoff, A. J., Eds.; Kluwer Academic Publishers: Dordrecht, Netherlands, 1996; p 255.
- (17) Norris, J. R.; Uphaus, R. A.; Crespi, H. L.; Katz, J. J. *Proc. Natl. Acad. Sci. USA* **1971**, *68*, 625. Davis, M. S.; Forman, A.; Fajer, J. *Proc. Natl. Acad. Sci. USA* **1979**, *76*, 4170. Kass, H.; Bittersmann-Weidlich, E.; Andreasson, L. E.; Bönigk, B.; Lubitz, W. *Chem. Phys.* **1995**, *194*, 419.